Throughput Performance Models for Adaptive Modulation and Coding under Fading Channels

Miguel López-Benítez
Dept. Electrical Engineering and Electronics
University of Liverpool, United Kingdom
Email: M.Lopez-Benitez@liverpool.ac.uk

***Abstract*—Modern wireless communication systems adapt the employed Modulation and Coding Scheme (MCS) to the instantaneous channel quality in order to maximise the amount of bits correctly transmitted per time unit (i.e., the throughput). An important aspect in the study of this technique, referred to as Adaptive Modulation and Coding (AMC), is the characterisation of the link throughput performance under realistic fading channels. In this context, this work derives analytically tractable closed-form expressions for the link throughput performance of AMC under Rayleigh, Nakagami-m, Nakagami-q (Hoyt), Nakagami-n (Rice), η-μ and κ-μ fading channels. The correctness and accuracy of the obtained expressions is corroborated numerically and with results from an LTE link level AMC simulator.**

***Index Terms*—Adaptive modulation and coding, link adaptation, throughput performance, fading channels, LTE.**

I. Introduction

A popular technique in modern digital wireless communication systems is Adaptive Modulation and Coding (AMC), which dynamically adapts the employed Modulation and Coding Scheme (MCS) to the instantaneous channel quality conditions. The optimum MCS is selected from a predefined set of available options, which are designed to provide varying levels of protection against radio propagation errors and transmission data rate. Several communication standards such as EDGE [1], HSDPA [2], LTE [3], IEEE 802.11 [4, 5], IEEE 802.15 [6–8] and IEEE 802.16 [9, 10], among others, have adopted AMC as a fundamental technique to optimise the link performance.

The method employed to select the optimum MCS is a key aspect in the design and resulting performance of AMC. Some existing solutions are based on the real-time monitoring of a particular metric (such as the short-term error rate or the short-term throughput) and the dynamic adaptation of the employed MCS in order to guarantee that the instantaneous values of the metric of interest fall within acceptable ranges so that a certain performance target in the long term (e.g., the long-term error rate or the long-term throughput) can be guaranteed. Some examples of this type of methods can be found in [2, 5–7, 11]. Alternatively, the MCS adaptation can be based on the real-time monitoring of the instantaneous channel quality, typically expressed in terms of the Signal-to-Noise Ratio (SNR). Each MCS is associated with a certain range of values of the instantaneous SNR, where it is optimum according to a predefined criterion, and selected whenever the instantaneous SNR falls within the associated interval. Such SNR intervals are determined by a set of SNR switching thresholds, which can be computed based on different criteria such as the throughput maximisation [2, 9–12] or the throughput maximisation subject to a maximum error rate [1, 9, 11, 13], among others.

An important aspect in the design and performance evaluation of AMC is the calculation of the link throughput under different fading channels for a predefined set of SNR thresholds. In this context, this work presents a simple approach to analytically derive closed-form expressions for the link throughput performance of AMC under fading channels. Based on the presented approach, analytically tractable closed-form expressions are derived for Rayleigh, Nakagami-m, Nakagami-q (Hoyt), Nakagami-n (Rice), η-μ and κ-μ fading channels. The ability of the obtained models to accurately predict the throughput performance is validated with results from an LTE link level AMC simulator developed to this end.

The rest of this work is organised as follows. First, Section II presents the considered system model and formulates the problem addressed in this paper. The procedure to obtain the exact result to the considered problem is then described in Section III. Given the intrinsic analytical difficulties of exact calculations, an approximated method is presented as an alternative in Section IV along with analytically tractable closed-form expressions for several fading channels. The correctness and accuracy of the obtained expressions are validated with results from an LTE link level AMC simulator developed to this end, the implementation of which is described in Section V. Performance results are presented and discussed in Section VI. Finally, Section VII summarises and concludes the paper.

II. System Model and Problem Formulation

Let N denote the number of MCS available in the system of interest. The nth MCS is characterised by a certain probability of error, denoted as $\varepsilon_n(\gamma)$, which depends on the instantaneous SNR, denoted as γ. Each MCS can transmit a different number of bits per modulated symbol (depending on the modulation order) and a different proportion of information/redundant bits (depending on the employed channel coding scheme). As a result, each MCS can transmit a different number of information bits per second, denoted as R_n, which represents the gross data rate of the nth MCS. For notation purposes, MCS are indexed such that $R_n < R_{n+1}$, $n = 1, \ldots, N-1$.

The employed MCS is dynamically adapted to the instantaneous SNR based on a set of SNR thresholds $\{\gamma_n^{th}\}_{n=1}^N$, which define the range of values of γ on which each MCS is used.

The nth MCS is selected whenever $\gamma \in [\gamma_n^{th}, \gamma_{n+1}^{th})$, except for the Nth MCS which is used in the interval $\gamma \in [\gamma_N^{th}, \infty)$.

The problem addressed in this work is the analytical derivation of closed-form expressions for the average link throughput under fading channels given the SNR thresholds $\{\gamma_n^{th}\}_{n=1}^{N}$.

III. EXACT CALCULATION

The throughput of an individual MCS as a function of the instantaneous SNR can be expressed as $\Gamma_n(\gamma) = R_n[1-\varepsilon_n(\gamma)]$. The average throughput of AMC under fading can be obtained by averaging $\Gamma_n(\gamma)$ for all MCS over the SNR statistics, taking into account the corresponding SNR range on which each MCS is used. The result can be expressed as:

$$\overline{\Gamma}(\overline{\gamma}) = \sum_{n=1}^{N-1} \overline{\Gamma}_n(\overline{\gamma}) + \overline{\Gamma}_N(\overline{\gamma}) \tag{1}$$

which depends on the average SNR, denoted as $\overline{\gamma}$, where:

$$\begin{aligned}\overline{\Gamma}_n(\overline{\gamma}) &= \int_{\gamma_n^{th}}^{\gamma_{n+1}^{th}} \Gamma_n(\gamma) f_\gamma(\gamma) d\gamma \\ &= R_n \left[\int_{\gamma_n^{th}}^{\gamma_{n+1}^{th}} f_\gamma(\gamma) d\gamma - \int_{\gamma_n^{th}}^{\gamma_{n+1}^{th}} \varepsilon_n(\gamma) f_\gamma(\gamma) d\gamma \right] \end{aligned}\tag{2}$$

$$\begin{aligned}\overline{\Gamma}_N(\overline{\gamma}) &= \int_{\gamma_N^{th}}^{\infty} \Gamma_N(\gamma) f_\gamma(\gamma) d\gamma \\ &= R_N \left[\int_{\gamma_N^{th}}^{\infty} f_\gamma(\gamma) d\gamma - \int_{\gamma_N^{th}}^{\infty} \varepsilon_N(\gamma) f_\gamma(\gamma) d\gamma \right] \end{aligned}\tag{3}$$

and $f_\gamma(\gamma)$ represents the Probability Density Function (PDF) of the instantaneous SNR per symbol. While $\varepsilon_n(\gamma)$ can be modelled using several proposed approximations (e.g., [14, eq. (3)], [15, eq. (5)] or [16, eq. (5)]), the integral of $\varepsilon_n(\gamma) f_\gamma(\gamma)$ is in general difficult to derive analytically (except for some particular combinations of error models and fading channels). As an alternative, an approximated simpler approach is considered in this work, which is described in Section IV.

IV. APPROXIMATED CALCULATION

In order to optimise the link performance, the SNR thresholds $\{\gamma_n^{th}\}_{n=1}^{N}$ should lead to the utilisation of each MCS on an interval of SNR values where its throughput is maximum, i.e., $\Gamma_n(\gamma) = R_n[1-\varepsilon_n(\gamma)] \approx R_n$, which implies that the corresponding SNR interval should lead to a low error probability, i.e., $\varepsilon_n(\gamma) \approx 0$. This approximation simplifies the integrals in (2) and (3) leading to:

$$\overline{\Gamma}(\overline{\gamma}) \approx \sum_{n=1}^{N} p_n(\overline{\gamma}) R_n \tag{4}$$

where $p_n(\overline{\gamma})$ represents the probability of selecting the nth MCS and depends on the fading characteristics of the channel:

$$p_n(\overline{\gamma}) = \begin{cases} \int_{\gamma_n^{th}}^{\gamma_{n+1}^{th}} f_\gamma(\gamma) d\gamma & n = 1, \ldots, N-1 \quad \text{(5a)} \\ \int_{\gamma_n^{th}}^{\infty} f_\gamma(\gamma) d\gamma & n = N \quad \text{(5b)} \end{cases}$$

which can alternatively be expressed in terms of the Cumulative Distribution Function (CDF) of the instantaneous SNR per symbol, denoted as $F_\gamma(\gamma)$:

$$p_n(\overline{\gamma}) = \begin{cases} F_\gamma(\gamma_{n+1}^{th}) - F_\gamma(\gamma_n^{th}) & n = 1, \ldots, N-1 \quad \text{(6a)} \\ 1 - F_\gamma(\gamma_n^{th}) & n = N \quad \text{(6b)} \end{cases}$$

The problem of calculating the average throughput of AMC, $\overline{\Gamma}(\overline{\gamma})$, then reduces to obtaining the probabilities of selection for each MCS, $p_n(\overline{\gamma})$, based on the channel fading statistics. Analytically tractable closed-form expressions for various fading channels are derived in the following sections.

A. Rayleigh fading

Under Rayleigh fading the instantaneous SNR per symbol is distributed according to [17, eq. (2.7)]:

$$f_\gamma(\gamma) = \frac{1}{\overline{\gamma}} \exp\left(-\frac{\gamma}{\overline{\gamma}}\right) \tag{7}$$

$$F_\gamma(\gamma) = 1 - \exp\left(-\frac{\gamma}{\overline{\gamma}}\right) \tag{8}$$

where $\overline{\gamma}$ is the average SNR. Hence, using (6) yields:

$$p_n(\overline{\gamma}) = \begin{cases} \exp\left(-\frac{\gamma_n^{th}}{\overline{\gamma}}\right) - \exp\left(-\frac{\gamma_{n+1}^{th}}{\overline{\gamma}}\right) & \text{(9a)} \\ \qquad n = 1, \ldots, N-1 & \\ \exp\left(-\frac{\gamma_n^{th}}{\overline{\gamma}}\right) \qquad n = N & \text{(9b)} \end{cases}$$

B. Nakagami-m fading

Under Nakagami-m fading the instantaneous SNR per symbol is distributed according to [17, eq. (2.21)]:

$$f_\gamma(\gamma) = \frac{m^m \gamma^{m-1}}{\overline{\gamma}^m \Gamma(m)} \exp\left(-\frac{m\gamma}{\overline{\gamma}}\right) \tag{10}$$

$$F_\gamma(\gamma) = P\left(m, \frac{m\gamma}{\overline{\gamma}}\right) = \frac{1}{\Gamma(m)} \int_0^{\frac{m\gamma}{\overline{\gamma}}} e^{-t} t^{m-1} dt \tag{11}$$

where $m \geq 1/2$ is the Nakagami-m fading parameter, $\Gamma(\cdot)$ is the gamma function [18, eq (6.1.1)] and $P(\cdot)$ is the regularised lower incomplete gamma function [18, eq. (6.5.1)]. Hence:

$$p_n(\overline{\gamma}) = \begin{cases} P\left(m, \frac{m\gamma_{n+1}^{th}}{\overline{\gamma}}\right) - P\left(m, \frac{m\gamma_n^{th}}{\overline{\gamma}}\right) & \text{(12a)} \\ \qquad n = 1, \ldots, N-1 & \\ 1 - P\left(m, \frac{m\gamma_n^{th}}{\overline{\gamma}}\right) \qquad n = N & \text{(12b)} \end{cases}$$

While the expression in (12) can be employed in numerical evaluations, its use in analytical manipulations can be difficult since $P(\cdot)$ is defined as a quotient of integrals. To overcome this drawback, an alternative closed-form expression with a more tractable algebraic form is here derived.

Introducing (10) into (5a) yields the following integral:

$$p_n(\overline{\gamma}) = \frac{m^m}{\overline{\gamma}^m \Gamma(m)} \int_{\gamma_n^{th}}^{\gamma_{n+1}^{th}} \gamma^{m-1} \exp\left(-\frac{m\gamma}{\overline{\gamma}}\right) d\gamma \tag{13}$$

The solution to the integral of (13) can be expressed in terms of the exponential integral [18, eq. (5.1.4)]; however, this would provide no advantage with respect to (12). An algebraically tractable expression can be obtained by solving the integral for integer values of m based on [18, eq (4.2.55)], which yields:

$$\widetilde{p}_n(\overline{\gamma}) = \exp\left(-\frac{m\gamma_n^{th}}{\overline{\gamma}}\right)\sum_{k=0}^{m-1}\frac{1}{k!}\left(\frac{m\gamma_n^{th}}{\overline{\gamma}}\right)^k - \exp\left(-\frac{m\gamma_{n+1}^{th}}{\overline{\gamma}}\right)\sum_{k=0}^{m-1}\frac{1}{k!}\left(\frac{m\gamma_{n+1}^{th}}{\overline{\gamma}}\right)^k \quad (14)$$
$$n = 1, \ldots, N-1$$

Similarly, introducing (10) into (5b) and following the same procedure yields the following result:

$$\widetilde{p}_n(\overline{\gamma}) = \exp\left(-\frac{m\gamma_n^{th}}{\overline{\gamma}}\right)\sum_{k=0}^{m-1}\frac{1}{k!}\left(\frac{m\gamma_n^{th}}{\overline{\gamma}}\right)^k \qquad n = N \quad (15)$$

The expressions in (14) and (15) have a more tractable algebraic form than (12), but are valid for integer values of $m \geq 1$ only. For any arbitrary (valid) $m \geq 1$, the corresponding result can be approximated by that of the nearest integer (i.e., $\lfloor m \rceil$) or obtained by interpolating between the nearest lower and higher integer values (i.e., $\lfloor m \rfloor$ and $\lceil m \rceil$, respectively):

$$p_n(\overline{\gamma}) = \widetilde{p}_n(\overline{\gamma})_{\lfloor m \rfloor} + \frac{m - \lfloor m \rfloor}{\lceil m \rceil - \lfloor m \rfloor}\left(\widetilde{p}_n(\overline{\gamma})_{\lceil m \rceil} - \widetilde{p}_n(\overline{\gamma})_{\lfloor m \rfloor}\right) \qquad m \geq 1 \quad (16)$$

where $\widetilde{p}_n(\overline{\gamma})_x$ denotes $\widetilde{p}_n(\overline{\gamma})$ evaluated in $m = x$. For $m < 1$ the interpolation in (16) is not valid because $m = 0$ is not a valid value for the m fading parameter. In such a case, other equivalent fading distributions can be used for $m \in [\frac{1}{2}, 1)$. For example, the η-μ (Section IV-E) and κ-μ (Section IV-F) distributions are equivalent to Nakagami-m when $\eta \to 0$ or $\eta \to \infty$ (Format 1) or $\eta \to \pm 1$ (Format 2) and $\kappa \to 0$, respectively; then μ becomes the m fading parameter.

C. Nakagami-q (Hoyt) fading

Under Nakagami-q (Hoyt) fading the instantaneous SNR per symbol is distributed according to [17, eq. (2.11)]:

$$f_\gamma(\gamma) = \frac{1+q^2}{2q\overline{\gamma}}\exp\left(-\frac{(1+q^2)^2}{4q^2}\frac{\gamma}{\overline{\gamma}}\right) I_0\left(\frac{1-q^4}{4q^2}\frac{\gamma}{\overline{\gamma}}\right) \quad (17)$$

where $q \in [0, 1]$ is the Nakagami-q fading parameter and $I_\nu(\cdot)$ is the νth-order modified Bessel function of the first kind [18, eq. (9.6.20)]. The associated CDF can be expressed in terms of the Marcum Q-function based on [19, eq. (8)], which can be introduced into (6) to obtain $p_n(\overline{\gamma})$. However, since the Marcum Q-function is defined as an integral, the expression obtained this way presents an algebraic form that is difficult to employ in analytical manipulations, which motivates the derivation of an alternative and tractable expression.

Employing [18, eq. (9.6.10)] and taking into account that $\Gamma(k+1) = k!$ the Bessel function $I_0(\cdot)$ can be written as:

$$I_0(x) = \sum_{k=0}^{\infty}\frac{\left(\frac{1}{2}x\right)^{2k}}{(k!)^2} \quad (18)$$

Introducing (17) and (18) into (5a) yields the sum of integrals:

$$p_n(\overline{\gamma}) = \frac{1+q^2}{2q\overline{\gamma}}\sum_{k=0}^{\infty}\frac{1}{(k!)^2}\left(\frac{1-q^4}{8q^2\overline{\gamma}}\right)^{2k} \times \int_{\gamma_n^{th}}^{\gamma_{n+1}^{th}}\gamma^{2k}\exp\left(-\frac{(1+q^2)^2}{4q^2}\frac{\gamma}{\overline{\gamma}}\right)d\gamma \quad (19)$$

The integral in (19) can be solved using [18, eq (4.2.55)]:

$$p_n(\overline{\gamma}) = \frac{2q}{1+q^2}\sum_{k=0}^{\infty}\left(\frac{1}{2}\frac{1-q^4}{(1+q^2)^2}\right)^{2k} \times \left[e^{-\frac{(1+q^2)^2}{4q^2}\frac{\gamma_n^{th}}{\overline{\gamma}}}\sum_{j=0}^{2k}\frac{(2k)!}{j!(k!)^2}\left(\frac{(1+q^2)^2}{4q^2}\frac{\gamma_n^{th}}{\overline{\gamma}}\right)^j - e^{-\frac{(1+q^2)^2}{4q^2}\frac{\gamma_{n+1}^{th}}{\overline{\gamma}}}\sum_{j=0}^{2k}\frac{(2k)!}{j!(k!)^2}\left(\frac{(1+q^2)^2}{4q^2}\frac{\gamma_{n+1}^{th}}{\overline{\gamma}}\right)^j\right] \quad (20)$$
$$n = 1, \ldots, N-1$$

Similarly, introducing (17) and (18) into (5b) yields:

$$p_n(\overline{\gamma}) = \frac{2q}{1+q^2}\sum_{k=0}^{\infty}\left(\frac{1}{2}\frac{1-q^4}{(1+q^2)^2}\right)^{2k} \times e^{-\frac{(1+q^2)^2}{4q^2}\frac{\gamma_n^{th}}{\overline{\gamma}}}\sum_{j=0}^{2k}\frac{(2k)!}{j!(k!)^2}\left(\frac{(1+q^2)^2}{4q^2}\frac{\gamma_n^{th}}{\overline{\gamma}}\right)^j \quad (21)$$
$$n = N$$

Notice that (20) and (21) are valid for any value of the q fading parameter (i.e., no interpolation is required).

D. Nakagami-n (Rice) fading

Under Nakagami-n (Rice) fading the instantaneous SNR per symbol is distributed according to [17, eq. (2.16)]:

$$f_\gamma(\gamma) = \frac{(1+K)e^{-K}}{\overline{\gamma}}\exp\left(-(1+K)\frac{\gamma}{\overline{\gamma}}\right) \times I_0\left(2\sqrt{K(1+K)\frac{\gamma}{\overline{\gamma}}}\right) \quad (22)$$

where $K = n^2$ is the Rician K factor, with $n \geq 0$ being the Nakagami-n fading parameter (K is here employed to avoid confusion with the MCS index n). The associated SNR CDF can be expressed in terms of the Marcum Q-function but the resulting expression for $p_n(\overline{\gamma})$ would be of little analytical utility. An analytically tractable expression is here derived.

Introducing (18) and (22) into (5a) yields:

$$p_n(\overline{\gamma}) = e^{-r^2}\sum_{k=0}^{\infty}\frac{K^k}{(k!)^2}\left(\frac{1+K}{\overline{\gamma}}\right)^{k+1} \times \int_{\gamma_n^{th}}^{\gamma_{n+1}^{th}}\gamma^k\exp\left(-(1+K)\frac{\gamma}{\overline{\gamma}}\right)d\gamma \quad (23)$$

Notice that (23) has the same algebraic form as (19). Hence:

$$p_n(\overline{\gamma}) = e^{-K}\sum_{k=0}^{\infty} K^k \times \Bigg[e^{-(1+K)\frac{\gamma_n^{th}}{\overline{\gamma}}} \sum_{j=0}^{k} \frac{1}{j!k!} \left((1+K)\frac{\gamma_n^{th}}{\overline{\gamma}} \right)^j - e^{-(1+K)\frac{\gamma_{n+1}^{th}}{\overline{\gamma}}} \sum_{j=0}^{k} \frac{1}{j!k!} \left((1+K)\frac{\gamma_{n+1}^{th}}{\overline{\gamma}} \right)^j \Bigg] \quad n = 1, \ldots, N-1 \tag{24}$$

Similarly, introducing (18) and (22) into (5b) yields:

$$p_n(\overline{\gamma}) = e^{-K}\sum_{k=0}^{\infty} K^k \times e^{-(1+K)\frac{\gamma_n^{th}}{\overline{\gamma}}} \sum_{j=0}^{k} \frac{1}{j!k!} \left((1+K)\frac{\gamma_n^{th}}{\overline{\gamma}} \right)^j \quad n = N \tag{25}$$

Notice that (24) and (25) are valid for any value of the K fading parameter (i.e., no interpolation is required).

E. η-μ fading

Under η-μ fading the instantaneous SNR per symbol is distributed according to [20, eq. (26)]:

$$f_\gamma(\gamma) = \frac{2\sqrt{\pi}\mu^{\mu+\frac{1}{2}}h^\mu}{\Gamma(\mu)H^{\mu-\frac{1}{2}}} \frac{\gamma^{\mu-\frac{1}{2}}}{\overline{\gamma}^{\mu+\frac{1}{2}}} \exp\left(-2\mu h\frac{\gamma}{\overline{\gamma}}\right) I_{\mu-\frac{1}{2}}\left(2\mu H\frac{\gamma}{\overline{\gamma}}\right) \tag{26}$$

where η and μ are the fading parameters, and h and H are functions of η (see [20] for details).

Introducing the following equality [18, eq. (9.6.10)]:

$$I_\nu(x) = \sum_{k=0}^{\infty} \frac{\left(\frac{1}{2}x\right)^{\nu+2k}}{k!\Gamma(\nu+k+1)} \tag{27}$$

into (26) and then into (5a) yields the sum of integrals:

$$p_n(\overline{\gamma}) = 2\sqrt{\pi}\sum_{k=0}^{\infty} \frac{\mu^{2\mu+2k}h^\mu H^{2k}}{\Gamma(\mu)\Gamma(\mu+k+\frac{1}{2})\overline{\gamma}^{2\mu+2k}} \frac{1}{k!} \times \int_{\gamma_n^{th}}^{\gamma_{n+1}^{th}} \gamma^{2\mu+2k-1} \exp\left(-2\mu h\frac{\gamma}{\overline{\gamma}}\right) d\gamma \tag{28}$$

Since μ represents half the number of multipath clusters, 2μ takes integer values and so does $2\mu+2k-1$ ($\mu > 0$). Based on [18, eq (4.2.55)], the integral in (28) can be solved for integer values of $2\mu + 2k - 1$, which yields the following result:

$$\widetilde{p}_n(\overline{\gamma}) = \sqrt{\pi}\sum_{k=0}^{\infty} \frac{H^{2k}}{\Gamma(\mu)\Gamma(\mu+k+\frac{1}{2})2^{2\mu+2k-1}h^{\mu+2k}} \times \Bigg[e^{-2\mu h\frac{\gamma_n^{th}}{\overline{\gamma}}} \sum_{j=0}^{2\mu+2k-1} \frac{(2\mu+2k-1)!}{j!k!} \left(2\mu h\frac{\gamma_n^{th}}{\overline{\gamma}}\right)^j - e^{-2\mu h\frac{\gamma_{n+1}^{th}}{\overline{\gamma}}} \sum_{j=0}^{2\mu+2k-1} \frac{(2\mu+2k-1)!}{j!k!} \left(2\mu h\frac{\gamma_{n+1}^{th}}{\overline{\gamma}}\right)^j \Bigg] \quad n = 1, \ldots, N-1 \tag{29}$$

Similarly, introducing (27) into (26) and then into (5b) yields:

$$\widetilde{p}_n(\overline{\gamma}) = \sqrt{\pi}\sum_{k=0}^{\infty} \frac{H^{2k}}{\Gamma(\mu)\Gamma(\mu+k+\frac{1}{2})2^{2\mu+2k-1}h^{\mu+2k}} \times e^{-2\mu h\frac{\gamma_n^{th}}{\overline{\gamma}}} \sum_{j=0}^{2\mu+2k-1} \frac{(2\mu+2k-1)!}{j!k!} \left(2\mu h\frac{\gamma_n^{th}}{\overline{\gamma}}\right)^j \quad n = N \tag{30}$$

The μ fading parameter is intended to be the *real* extension of half the number of multipath clusters, but in practice μ may differ from integer multiples of $1/2$ for a number of reasons [20]. For non-integer values of 2μ, the corresponding result can be approximated by that of the nearest integer (i.e., $\lfloor 2\mu \rceil$) or obtained by interpolating between the nearest lower and higher integer values (i.e., $\lfloor 2\mu \rfloor$ and $\lceil 2\mu \rceil$, respectively):

$$p_n(\overline{\gamma}) = \widetilde{p}_n(\overline{\gamma})_{\frac{\lfloor 2\mu \rfloor}{2}} + \frac{2\mu - \lfloor 2\mu \rfloor}{\lceil 2\mu \rceil - \lfloor 2\mu \rfloor} \left(\widetilde{p}_n(\overline{\gamma})_{\frac{\lceil 2\mu \rceil}{2}} - \widetilde{p}_n(\overline{\gamma})_{\frac{\lfloor 2\mu \rfloor}{2}} \right) \tag{31}$$

where $\widetilde{p}_n(\overline{\gamma})_x$ denotes $\widetilde{p}_n(\overline{\gamma})$ evaluated in $\mu = x$.

F. κ-μ fading

Under κ-μ fading the instantaneous SNR per symbol is distributed according to [20, eq. (10)]:

$$f_\gamma(\gamma) = \frac{\mu(1+\kappa)^{\frac{\mu+1}{2}}}{\kappa^{\frac{\mu-1}{2}}\exp(\mu\kappa)} \frac{\gamma^{\frac{\mu-1}{2}}}{\overline{\gamma}^{\frac{\mu+1}{2}}} \times \exp\left(-\mu(1+\kappa)\frac{\gamma}{\overline{\gamma}}\right) I_{\mu-1}\left(2\mu\sqrt{\kappa(1+\kappa)\frac{\gamma}{\overline{\gamma}}}\right) \tag{32}$$

where $\kappa, \mu > 0$ are fading parameters (see [20] for details).

Introducing (27) into (32) and then into (5a) yields:

$$p_n(\overline{\gamma}) = \sum_{k=0}^{\infty} \frac{\mu^{\mu+2k}\kappa^k(1+\kappa)^{\mu+k}}{\exp(\mu\kappa)\,\overline{\gamma}^{\mu+k}} \frac{1}{k!(\mu+k-1)!} \times \int_{\gamma_n^{th}}^{\gamma_{n+1}^{th}} \gamma^{\mu+k-1} \exp\left(-\mu(1+\kappa)\frac{\gamma}{\overline{\gamma}}\right) d\gamma \tag{33}$$

Since μ represents the number of multipath clusters, μ takes integer values and so does $\mu+k-1$ ($\mu > 0$). Based on [18, eq

(4.2.55)], the integral in (33) can be solved for integer values of $\mu + k - 1$, which leads to the following result:

$$\widetilde{p}_n(\overline{\gamma}) = \sum_{k=0}^{\infty} (\mu\kappa)^k e^{-\mu\kappa} \tag{34}$$

$$\times \left[e^{-\mu(1+\kappa)\frac{\gamma_n^{th}}{\overline{\gamma}}} \sum_{j=0}^{\mu+k-1} \frac{1}{j!k!} \left(\mu(1+\kappa)\frac{\gamma_n^{th}}{\overline{\gamma}} \right)^j \right.$$

$$\left. - e^{-\mu(1+\kappa)\frac{\gamma_{n+1}^{th}}{\overline{\gamma}}} \sum_{j=0}^{\mu+k-1} \frac{1}{j!k!} \left(\mu(1+\kappa)\frac{\gamma_{n+1}^{th}}{\overline{\gamma}} \right)^j \right]$$

$$n = 1, \ldots, N-1$$

Similarly, introducing (27) into (32) and then into (5b) yields:

$$\widetilde{p}_n(\overline{\gamma}) = \sum_{k=0}^{\infty} (\mu\kappa)^k e^{-\mu\kappa} \tag{35}$$

$$\times\, e^{-\mu(1+\kappa)\frac{\gamma_n^{th}}{\overline{\gamma}}} \sum_{j=0}^{\mu+k-1} \frac{1}{j!k!} \left(\mu(1+\kappa)\frac{\gamma_n^{th}}{\overline{\gamma}} \right)^j$$

$$n = N$$

The μ fading parameter is intended to be the *real* extension of the number of multipath clusters, but in practice μ may not be integer for a number of reasons [20]. The result for non-integer values of μ can be approximated by that of the nearest integer (i.e., $\lfloor\mu\rceil$) or obtained by interpolating between the nearest lower/higher integers (i.e., $\lfloor\mu\rfloor$ and $\lceil\mu\rceil$, respectively):

$$p_n(\overline{\gamma}) = \widetilde{p}_n(\overline{\gamma})_{\lfloor\mu\rfloor} + \frac{\mu - \lfloor\mu\rfloor}{\lceil\mu\rceil - \lfloor\mu\rfloor} \left(\widetilde{p}_n(\overline{\gamma})_{\lceil\mu\rceil} - \widetilde{p}_n(\overline{\gamma})_{\lfloor\mu\rfloor} \right) \tag{36}$$

where $\widetilde{p}_n(\overline{\gamma})_x$ denotes $\widetilde{p}_n(\overline{\gamma})$ evaluated in $\mu = x$.

V. Simulation Method

The throughput performance of AMC is evaluated based on the simulation method of Fig. 1. For evaluation purposes the LTE MCS are considered. The curves for the error probabilities $\{\varepsilon_n(\gamma)\}_{n=1}^N$ are obtained from [21, Fig. 5], which are also employed to compute the set of SNR thresholds $\{\gamma_n^{th}\}_{n=1}^N$ so that a maximum error probability of 0.1 is not exceeded [22, Sect. 7.2.3]. The gross data rates $\{R_n\}_{n=1}^N$ are computed at the Physical Resource Block (PRB) level (12 subcarriers) considering a normal cyclic prefix (14 OFDM symbols per 1-ms subframe and subcarrier) based on [22, Table 7.2.3-1]. Other simulation inputs are the number of simulated subframes ($N_s = 10000$) and the subframe duration ($T_s = 0.001$ s).

For each of the N_s simulated subframes, an instantaneous SNR value γ_s is generated as a random number drawn from the selected fading distribution $f_\gamma(\gamma)$. If $\gamma_s < \gamma_1^{th}$ no transmission is performed; otherwise a transmission is performed using the MCS, i, that is optimum for the current γ_s. The transmission result is decided by comparing a random number uniformly distributed in $[0,1]$, $U(0,1)$, with the error probability of the selected MCS for the current SNR, $\varepsilon_i(\gamma_s)$. If the transmission is successful, the counter for the total number of correctly transmitted bits, N_b, is increased by the number of bits

Input: $\{\gamma_n^{th}\}_{n=1}^N$, $\{\varepsilon_n(\gamma)\}_{n=1}^N$, $\{R_n\}_{n=1}^N$, $N_s \in \mathbb{N}^+$, $T_s > 0$
Output: $\overline{\Gamma}(\overline{\gamma})$

$N_b = 0$ {Number of bits correctly transmitted}
for N_s subframes **do**
  Randomly generate the instantaneous SNR: $\gamma_s \sim f_\gamma(\gamma)$
  if $\gamma_s \geq \gamma_1^{th}$ **then**
    if $\gamma_s \geq \gamma_N^{th}$ **then**
      Select the MCS as $i = N$
    else
      Select the MCS as $i = \{n : \gamma_n^{th} \leq \gamma_s < \gamma_{n+1}^{th}\}$
    end if
    if $U(0,1) > \varepsilon_i(\gamma_s)$ **then**
      $N_b = N_b + T_s R_i$
    end if
  end if
end for
$\overline{\Gamma}(\overline{\gamma}) = N_b / N_s T_s$

Fig. 1. Simulation method.

transmitted in that subframe, $T_s R_i$. The average throughput is obtained as the quotient between the total number of correctly transmitted bits, N_b, and the simulated time, $N_s T_s$.

VI. Performance Results

Fig. 2 illustrates the LTE link throughput performance (in megabits per second per LTE PRB) as a function of the average SNR for various fading scenarios. Exact numerical results (represented by lines) have been obtained based on (1) and the numerical calculation of the integrals in (2) and (3), where the curves for the error probabilities $\{\varepsilon_n(\gamma)\}_{n=1}^N$ are obtained from [21, Fig. 5]. Analytical results (represented by circles) have been obtained based on (4) and the expressions analytically derived for $p_n(\overline{\gamma})$ in Sections IV-A to IV-F. Simulation results (represented by dots) have been obtained based on the simulation procedure described in Section V.

Fig. 2(a) shows the LTE throughput performance under Rayleigh and Nakagami-m fading (notice that both are equivalent for $m = 1$). As appreciated, the obtained analytical expressions provide an accurate prediction of the throughput performance for the whole range of average SNR values. The detail of Fig. 2(a) indicates that, for non-integer values of the Nakagami-m fading parameter (e.g., $m = 1.5$), rounding to an integer value of m (i.e., $m = 1$ or $m = 2$) may not provide an adequate level of accuracy. However, the interpolation proposed in (16) provides an accurate approximation to the exact value. Although this interpolation approach is valid for $m \geq 1$ only, other equivalent fading distributions can be used for $m \in [\frac{1}{2}, 1)$. As discussed in Section IV-B, the η-μ and κ-μ distributions embrace Nakagami-m as a particular case. The performance expressions for these distributions and their associated interpolations in (31) and (36) have no restrictions and, as appreciated in Fig. 2(c), provide a remarkable level of accuracy, as it is also the case for Nakagami-q/n in Fig. 2(b). The obtained results therefore demonstrate the accuracy of the expressions analytically derived in this paper.

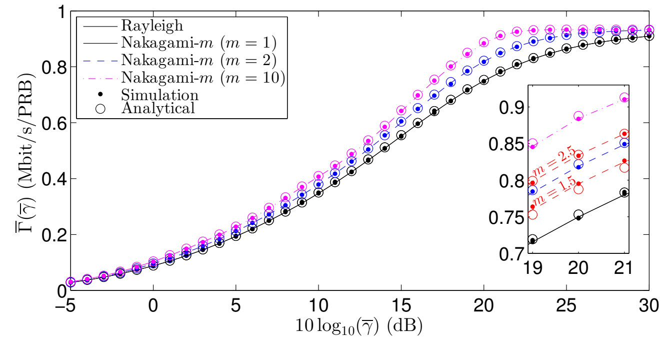

(a) Rayleigh and Nakagami-m fading

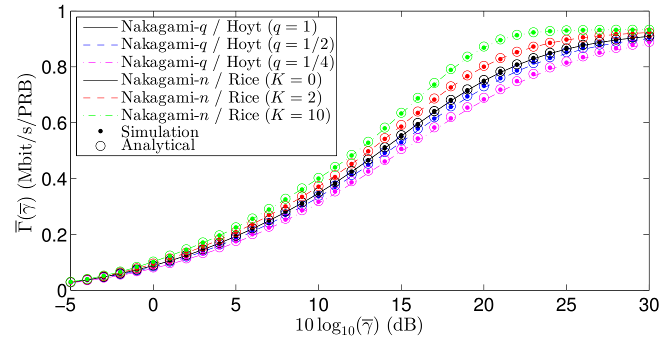

(b) Nakagami-q (Hoyt) and Nakagami-n (Rice) fading

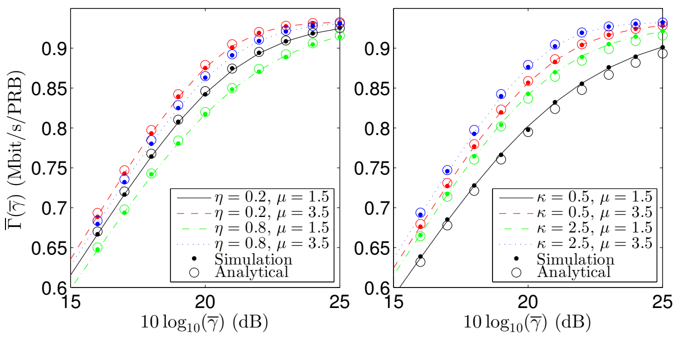

(c) η-μ Format 2 (left) and κ-μ (right) fading

Fig. 2. Numerical, analytical and simulated LTE throughput performance as a function of the average SNR for various fading scenarios.

VII. Conclusions

An important aspect in the study of AMC is the characterisation of the throughput performance under fading. This work has derived closed-form expressions for the throughput performance of AMC under Rayleigh, Nakagami-m, Nakagami-q (Hoyt), Nakagami-n (Rice), η-μ and κ-μ fading channels. The obtained expressions, which characterise the throughput in terms of the SNR switching thresholds, average SNR and fading parameters, are based on power and exponential functions and are therefore suitable for analytical manipulations. The comparison with exact numerical and simulation results demonstrates that the expressions derived in this paper provide an accurate characterisation of the link throughput performance of AMC under a wide range of fading scenarios.

References

[1] K. K. Leung, P. F. Driessen, K. Chawla, and X. Qiu, "Link adaptation and power control for streaming services in EGPRS wireless networks," *IEEE J. Sel. Areas Commun.*, vol. 19, no. 10, pp. 2029–2039, Oct. 2002.

[2] T. Cui, F. Lu, V. Sethuraman, A. Goteti, S. P. N. Rao, and P. Subrahmanya, "Throughput optimization in high speed downlink packet access (HSDPA)," *IEEE Trans. Wireless Commun.*, vol. 10, no. 2, pp. 474–483, Feb. 2011.

[3] G. Ku and J. Walsh, "Resource allocation and link adaptation in LTE and LTE advanced: a tutorial," *IEEE Commun. Surveys Tuts.*, vol. 17, no. 3, pp. 1605–1633, Dec. 2014.

[4] D. Qiao, S. Choi, and K. G. Shin, "Goodput analysis and link adaptation for IEEE 802.11a wireless LANs," *IEEE Trans. Mobile Comput.*, vol. 1, no. 4, pp. 278–292, Oct. 2002.

[5] P. Chevillat, J. Jelitto, A. N. Barreto, and H. Truong, "A dynamic link adaptation algorithm for IEEE 802.11 a wireless LANs," in *Proc. IEEE Int'l. Conf. Commun. (ICC 2003)*, vol. 2, United States, May 2003, pp. 1141–1145.

[6] F. Martelli, R. Verdone, and C. Buratti, "Link adaptation in IEEE 802.15.4-based wireless body area networks," in *Proc. 21st IEEE Int'l. Symp. Pers., Indoor and Mobile Radio Commun. (PIMRC 2010)*, Turkey, Sep. 2010, pp. 117–121.

[7] ——, "Link adaptation in wireless body area networks," in *Proc. 73rd IEEE Veh. Technol. Conf. (VTC 2011 Spring)*, Japan, May 2011, pp. 1–5.

[8] M. S. Mohammadi, E. Dutkiewicz, Q. Zhang, and X. Huang, "Optimal energy efficiency link adaptation in IEEE 802.15.6 IR-UWB body area networks," *IEEE Commun. Lett.*, vol. 18, no. 12, pp. 2193–2196, Dec. 2014.

[9] D. Marabissi, D. Tarchi, R. Fantacci, and F. Balleri, "Efficient adaptive modulation and coding techniques for WiMAX systems," in *Proc. IEEE Int'l. Conf. Commun. (ICC 2008)*, China, May 2008, pp. 3383–3387.

[10] C. Mehlführer, S. Caban, and M. Rupp, "Experimental evaluation of adaptive modulation and coding in MIMO WiMAX with limited feedback," *EURASIP Journal on Advances in Signal Processing*, vol. 2008, no. 837102, pp. 1–12, Jan. 2008.

[11] M. López-Benítez and J. Gozálvez, "Link adaptation algorithms for improved delivery of delay- and error-sensitive packet-data services over wireless networks," *Wireless Networks*, vol. 16, no. 3, pp. 593–606, Apr. 2010.

[12] X. Qiu and J. Chuang, "Link adaptation in wireless data networks for throughput maximization under retransmissions," in *Proc. IEEE Int'l. Conf. Commun. (ICC 1999)*, vol. 2, Canada, Jun. 1999, pp. 1272–1277.

[13] K. Manolakis, M. A. Gutiérrez-Estévez, and V. Jungnickel, "Adaptive modulation and turbo coding for 3GPP LTE systems with limited feedback," in *Proc. 79th IEEE Veh. Technol. Conf. (VTC 2014 Spring)*, Republic of Korea, May 2014, pp. 1–5.

[14] K. J. Hole, H. Holm, and G. E. Øien, "Adaptive multidimensional coded modulation over flat fading channels," *IEEE J. Sel. Areas Commun.*, vol. 18, no. 7, pp. 1153–1158, Jul. 2000.

[15] Q. Liu, S. Zhou, and G. B. Giannakis, "Cross-layer combining of adaptive modulation and coding with truncated ARQ over wireless links," *IEEE Trans. Wireless Commun.*, vol. 3, no. 5, pp. 1746–1755, Sep. 2004.

[16] H. Khodakarami and F. Lahouti, "Link adaptation for physical layer security over wireless fading channels," *IET Communications*, vol. 6, no. 3, pp. 353–362, Feb. 2012.

[17] M. K. Simon and M.-S. Alouini, *Digital communications over fading channels*, 2nd ed. Wiley-IEEE Pres, 2005.

[18] M. Abramowitz and I. A. Stegun, *Handbook of mathematical functions with formulas, graphs, and mathematical tables*, 10th ed. Dover, 1972.

[19] J. F. Paris, "Nakagami-q (Hoyt) distribution function with applications," *Electron. Lett.*, vol. 45, no. 4, pp. 210–211, Feb. 2009.

[20] M. D. Yacoub, "The κ-μ distribution and the η-μ distribution," *IEEE Antennas Propag. Mag.*, vol. 49, no. 1, pp. 68–81, Feb. 2007.

[21] C. Mehlführer, M. Wrulich, J. C. Ikuno, D. Bosanska, and M. Rupp, "Simulating the long term evolution physical layer," in *Proc. 17th European Signal Processing Conf. (EUSIPCO 2009)*, United Kingdom, Aug. 2009, pp. 1471–1478.

[22] 3rd Generation Partnership Project, "Technical Specification Group Radio Access Network; Evolved Universal Terrestrial Radio Access (E-UTRA); Physical layer procedures (Release 12)," Tech. Rep. 3GPP TS 36.213, Dec. 2014, v12.4.0.